Manuscript

Determination of an architectural arch's geometry: the case of Palau Güell by Antoni Gaudí.

Abstract

We provide a method to objectively determine which is the geometric shape which best fits an arch of a heritage building within each of the conical curve types and hyperbolic curve types, and we also provide an objective measurement of that fit. This method does not involve mechanical, constructive or structural processes; it only involves standard geometric processes, numerical processes, computing, statistics and 3D data acquisition. Using these techniques we generate a method which allows an objective determination of an arch's geometry in a heritage building. For architectural and historical reasons, and also due to discrepancies regarding the arch's geometry, as an application case for this method we have chosen the arch on the façade of Palau Güell (1886-1890) in Barcelona, a heritage building designed by Antoni Gaudí.

Keywords

Architectural arch, geometric determination, Palau Güell, conics, catenary, Rankine.

Research Aims

We provide a method to objectively determine which is the geometric shape which best fits an arch of a heritage building within each of the conical curve types and hyperbolic curve types.

1. Introduction

Arches have been used in many ways and applied to different composition styles over time in architectural heritage buildings. Sometimes their geometric and constructive layout has been recorded on historical treatises or sketches which have survived to the present day, allowing us to know the construction process used by the architect to design that structural element [1]. But in other cases there are no documents to objectively determine the geometry used on the arches of prominent buildings. In such cases, a –subjective and intuitive– debate is usually opened in order to define the arch geometry, leading to discrepancies or even without coming to a clear conclusion.

This paper provides a method to objectively determine which is the geometric shape which best fits an arch of a heritage building within each of the conical curve types and hyperbolic curve types, and also provides an objective measurement of that fit. We say in advance that this method does not involve mechanical, constructive or structural processes; it only involves standard geometric processes, numerical processes, computing, statistics and 3D data acquisition.

This method is presented by means of an application case. Specifically, we will apply our method to the arch on the façade of Palau Güell (1886-1890) in Barcelona, a heritage building designed by Antoni Gaudí (Figure 1). This application example is remarkable for the following reasons:

1.- This is one the Gaudí's first buildings, where he experimented with several arch types and also delved into the complexities of architectural space and its relationships with natural light.

2.- There has been no agreement to date between experts on the type of such arch. In the official archives of Palau Güell there is only an illustrative elevation view and the corresponding floor plans of the building, but these documents are not enough to draw any geometric or architectural conclusions.

3.- There is no rigorous geometric analysis determining the type of arch.

Fig. 1. Study arch to which our geometric analysis method is applied.

The geometric and formal disagreement as to this arch's type has been portrayed on several publications, notably:

a) The author of the book entitled *Gaudí, búsqueda de la forma: espacio, geometría, estructura y construcción* claims on pages 34, 97-99 that the arch on the façade of Palau Güell is a catenary, but he also claims on pages 64, 83 and 136 that the same arch is a parabola. In addition to contradicting himself, he does not say which particular catenary or parabola that is, neither does he provide any proof of his claims [2].

b) The author of the communication entitled *La organización constructiva del descenso de cargas del Palau Güell de Barcelona, obra de Antoni Gaudí*, from the Third National Congress on the History of Construction (Tercer Congreso Nacional de Historia de la Construcción), concludes that the study arch is either a funicular arch or a catenary arch. In this case there is no contradiction, but, again, we are faced with uncertainty and lack of specificity about the arch geometry [3].

c) The author of the publication entitled *El Palau Güell de Antoni Gaudí en Barcelona* concludes on pages 48-55 that the study arch has a parabolic geometry. Just like the previous authors, he does not provide any verification in support of that claim, and he does not say which parabola is that [4].

d) The author of the publication entitled *Structural design in the work of Gaudí* concludes on page 326 that the geometry of the study arch "is very similar to" a Rankine curve. Nevertheless, he does not say how close that similarity is, and the particular Rankine curve is not mentioned either [5].

None of the aforementioned works [2-5] specifies the particular curve of the arches built on the entrance to the Palau Güell. All these studies provide –at the most– assumptions based on the lessons learnt by Gaudí during his student years (1873-1878) with regard to theories of thrust and the integration of those theories on architectural designs. And even though study [5] does provide some structural reasonings in support of the "similarity" claim, it does not provide any calculations or results with regard to the particular curve and the measure of that similarity. This ambiguity concerning one of the most remarkable buildings designed by Gaudí, together with the fact that there is no original document stating the particular type of arch, has led us to use this arch as an example, in order to provide a precise and rigorous answer. The analysis provided by this method is applicable to any architectural arch, finding the best fit within each of the conical curve types and hyperbolic curve types.

2. Method to determine an architectural arch's geometry

2.1. Geometric determination

Let $\mathcal{N}' = \{P'_i\}_{i=1}^{i=50155}$ be the point cloud outlining the edge contour of the door on the façade of Palau Güell. These points were obtained using photogrammetrical techniques and the software PhotoScan. For these points, we use 3D coordinates (x', y', z') according to the 3D orthonormal coordinate system $C' = \{p_1; \vec{u}_1, \vec{u}_2, \vec{u}_3\}$ of the scanning device (Figures 2 and 3).

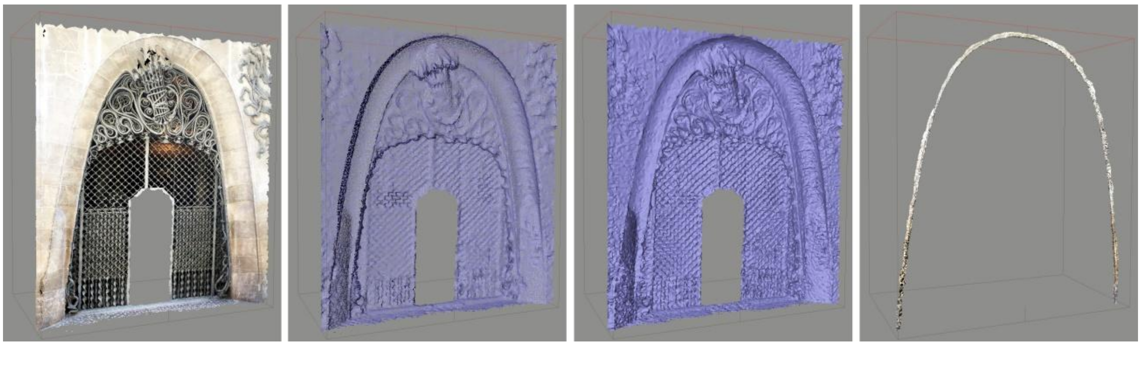

Fig. 2. Three-dimensional model of the study object created with PhotoScan software. The image on the far right shows the 50155 points which make up the edge contour of the study arch.

Fig. 3. Outline of the three-dimensional model of the study object created with PhotoScan software. The edge contour of the study arch is highlighted in red.

The geometric determination process starts with any three unaligned points on the façade. The coordinates of the three points chosen by us are as follows: ${P'}_1(5.9279, -8.4696, 14.2107)$; ${P'}_2(0.3369, -3.7996, 7.1161)$ and ${P'}_3(7.0906, -5.5039, 5.0833)$. The plane σ of the façade has the following equation: $\sigma \equiv 21.5846x' + 59.2802y' + 22.0108z' + 61.3384 = 0$

Given any arbitrary point ${P'}_i = (p_{1i}, p_{2i}, p_{3i})$ with coordinates on C', being $Q_i = (q_{1i}, q_{2i}, q_{3i})$ its foot on σ, i.e., the point resulting from the orthogonal projection on σ, we find that: $q_{1i} = 0.8956p_{1i} - 0.2866p_{2i} - 0.1064p_{3i} - 0.2965$; $q_{2i} = -0.2866p_{1i} + 0.2128p_{2i} - 0.2922p_{3i} - 0.8144$ and $q_{3i} = -0.1064p_{1i} - 0.2922p_{2i} + 0.8914p_{3i} - 0.3024$.

An orthonormal reference system $\mathcal{R}$ on the plane σ, generated from ${P'}_1, {P'}_2, {P'}_3$, is: $\mathcal{R} = \{p_1; \vec{v}_1, \vec{v}_2\}$; where $\vec{v}_1 = (-0.5498, 0.4592, -0.6976)$ and $\vec{v}_2 = (-0.7702, -0.0442, -0.6361)$.

The coordinates (a_i, b_i) of $P_i = Q_i + 10\vec{v}_1$ in $\mathcal{R}$, after calculation, are: $a_i = 0.1343q_{1i} + 2.3383q_{2i} + 29.0081$ and $b_i = 1.3941q_{1i} + 1.6690q_{2i} + 5.8721$. The summand $10\vec{v}_1$ has the purpose to move the point cloud $\{Q_i\}_{i=1}^{i=50155}$ away from the origin of the coordinate system.

The points on σ in the system $\mathcal{R}$ have coordinates $(\bar{x}, \bar{y})$; therefore, in the system $\mathcal{R}$, the equation of the conical regression curve ε for the point cloud $\{Q_i + 10\vec{v}_1\}_{i=1}^{i=50155}$ on plane σ is: $0 = B\bar{x}^2 + C\bar{y}^2 + D\bar{x}\bar{y} + E\bar{x} + F\bar{y} + 1$, where: $B = 0.0051$, $C = 0.0114$, $D = -0.0081$, $E = -0.1511$, $F = 0.0829$.

This conical regression curve $\varepsilon \equiv B\bar{x}^2 + C\bar{y}^2 + D\bar{x}\bar{y} + E\bar{x} + F\bar{y} + 1 = 0$ is the one which best fits the point cloud $\{Q_i + 10\vec{v}_1\}_{i=1}^{i=50155}$, minimizing the sum of the quadratic residues $\sum_{i=1}^{i=50155} \bar{\varepsilon}_i^2 = \sum_{i=1}^{i=50155}(Ba_i^2 + Cb_i^2 + Da_ib_i + Ea_i + Fb_i + 1)^2$. Eqs. (1) below are the Gauss normal equations which provide the solution to the calculation problem of ε. This equations have a range of variation 1–50155 in Einstein summation convention –throughout our paper we will use Einstein summation convention–, being $1_i = 1$.

$$\begin{pmatrix} 1_i a_i^4 & a_i^2 b_i^2 & a_i^3 b_i & 1_i a_i^3 & a_i^2 b_i \\ a_i^2 b_i^2 & 1_i b_i^4 & a_i b_i^3 & a_i b_i^2 & 1_i b_i^3 \\ a_i^3 b_i & a_i b_i^3 & a_i^2 b_i^2 & a_i^2 b_i & a_i b_i^2 \\ 1_i a_i^3 & a_i b_i^2 & a_i^2 b_i & 1_i a_i^2 & a_i b_i \\ a_i^2 b_i & 1_i b_i^3 & a_i b_i^2 & a_i b_i & 1_i b_i^2 \end{pmatrix} \begin{pmatrix} B \\ C \\ D \\ E \\ F \end{pmatrix} = \begin{pmatrix} -1_i a_i^2 \\ -1_i b_i^2 \\ -a_i b_i \\ -1_i a_i \\ -1_i b_i \end{pmatrix} \quad (1)$$

We find that the conical curve ε is an ellipse. The geometric elements of this ellipse in the system $\mathcal{R}$ are as follows:

- Center $\equiv \theta = (17.4313, 2.6951)$

- Major axis $\equiv (\bar{x}, \bar{y}) = \theta + \lambda \vec{e}_2$ where $\lambda \in \mathbb{R}$and $\vec{e}_2 = (-0.8963, -0.4433)$

- Minor axis $\equiv (\bar{x}, \bar{y}) = \theta + \lambda \vec{e}_1$ where $\lambda \in \mathbb{R}$ and $\vec{e}_1 = (-0.4433, 0.8963)$

As a result, we have the following orthonormal reference system $C = \{\theta;\ \vec{e}_1, \vec{e}_2\}$ for plane σ. The points on σ in the system C have coordinates $(\hat{x}, \hat{y})$. The coordinates $(\hat{x}_{i,} \hat{y}_i)$ of $\{P_i\}_{i=1}^{i=50155}$ in system C are: $\hat{x}_i = -0.4433 a_i + 0.8936 b_i + 5.3125$ and $\hat{y}_i = -0.8963 a_i - 0.4433 b_i + 16.8193$.

Thus, we have the point cloud $\mathcal{N} = \{P_i\}_{i=1}^{i=50155}$, which is a displacement of the orthogonal projection of cloud $\mathcal{N}' = \{P'_i\}_{i=1}^{i=50155}$ on the plane σ of the façade. In the reference system C, the points have coordinates $P_i = (\hat{x}_i, \hat{y}_i)$, so that the axis $\hat{Y} = \theta + \lambda \vec{e}_2$ is the central axis of the point cloud $\mathcal{N}$, as shown in Figure 4.

Next, we will find a subset of $\mathcal{N}$ which defines a point cloud for the edge of the access door to Palau Güell. To that effect, we produce an equispaced partition $\{(r_j, r_j + 1)\}_{j=1}^{j=100}$ of the range of variable $\hat{x}$ for the points P_i in $\mathcal{N}$ with 100 intervals, and we take the point $P_{i_j} = (\hat{x}_{i_j}, \hat{y}_{i_j}) \in \mathcal{N}$ such that $\hat{y}_{i_j} = \underset{\substack{i=1 \div 50155 \\ \hat{x}_i \in (r_j, r_{j+1})}}{\text{mín}} \{\hat{y}_i\}$. Thus we obtain a cloud $\mathcal{B} = \{P_{i_j}\}_{i_j=1}^{i_j=100}$ made up by 100 points in $\mathcal{N}$ which define the edge of the access door, having coordinates $P_{i_j} = (\hat{x}_{i_j}, \hat{y}_{i_j})$ in the reference system C (Figure 4).

Next we normalize the coordinates of the edge cloud $\mathcal{B}$. To that effect, we impose the condition that the lowest point in $\mathcal{B}$, having coordinates $(3.6898, -1.4305)$ in system C, must have coordinates (1,0). This normalization is the equivalent of a change of coordinates to the new reference system $\mathcal{G} = \{\mathcal{v}; \vec{n}_1, \vec{n}_2\}$, where: $\mathcal{v} = \theta + (0, -1.4305)$; $\vec{n}_1 = 3.6898\, \vec{e}_1$ and $\vec{n}_2 = 3.6297\, \vec{e}_2$.

The points on σ in the system $\mathcal{G}$ have coordinates (x, y). The coordinates (x_{i_j}, y_{i_j}) of $\{P_{i_j}\}_{i_j=1}^{i_j=100}$ in system $\mathcal{G}$ are: $x_{i_j} = 0.2710 \hat{x}_{i_j}$ and $y_{i_j} = 0.2710 \hat{y}_{i_j} + 0.3876$.

After defining the final reference system $\mathcal{G}$ –which, as we have seen, originates from the conical regression curve ε as a result from geometric transformations of the cloud $\mathcal{N}'$, and therefore is an intrinsic system of the cloud itself–, we will find the conical regression curves and hyperbolic regression curves for the point cloud $\mathcal{B}$ of the door's edge, obtaining their equations in the system $\mathcal{G}$.

We calculate **P**, the parabola regression curve of $\mathcal{B}$, and we obtain the following equation Eq. (2) in the reference system $\mathcal{G}$ (Figure 4):

$$\mathbf{P} \equiv y = Ax^2 + B \text{ where } \begin{cases} A = -2.0678 \\ B = 2.7074 \end{cases} \quad (2)$$

This parabola regression curve $\mathbf{P} \equiv y = Ax^2 + B$ is the one which best fits the point cloud $\mathcal{B} = \left\{P_{i_j}\right\}_{i_j=1}^{i_j=100}$, minimizing the sum of the quadratic residues $\sum_{i_j=1}^{i_j=100} \varepsilon_{pi_j}^2 = \sum_{i_j=1}^{i_j=100} \left(Ax_{i_j}^2 + B - y_{i_j}\right)^2$. Eqs. (3) below are the Gauss normal equations which provide the solution to the calculation problem of **P**. This equations have a range of variation 1–100 in Einstein summation convention, being $1_{i_j} = 1$.

$$\begin{pmatrix} 1_{i_j}x_{i_j}^4 & 1_{i_j}x_{i_j}^2 \\ 1_{i_j}x_{i_j}^2 & 1_{i_j}1_{i_j} \end{pmatrix} \begin{pmatrix} A \\ B \end{pmatrix} = \begin{pmatrix} x_{i_j}^2 y_{i_j} \\ 1_{i_j} y_{i_j} \end{pmatrix} \qquad (3)$$

Similarly, we calculate **E**, the ellipse regression curve of $\mathcal{B}$, and we obtain the following equation Eq. (4) in the reference system $\mathcal{G}$ (Figure 4):

$$\mathbf{E} \equiv y = \frac{1}{2}F \pm \frac{1}{2}\sqrt{F^2 + 4Bx^2 + 4G}, B < 0 \text{ where } \begin{cases} B = -5.3213 \\ F = 0.6657 \\ G = 4.9338 \end{cases} \qquad (4)$$

This ellipse regression curve $\mathbf{E} \equiv y = \frac{1}{2}F \pm \frac{1}{2}\sqrt{F^2 + 4Bx^2 + 4G}, B < 0$ is the one which best fits the point cloud $\mathcal{B} = \left\{P_{i_j}\right\}_{i_j=1}^{i_j=100}$, minimizing the sum of the quadratic residues $\sum_{i_j=1}^{i_j=100} \varepsilon_{ei_j}^2 = \sum_{i_j=1}^{i_j=100} \left(B'x_{i_j}^2 + C'y_{i_j}^2 + F'y_{i_j} + 1\right)^2, B'C' < 0$, $B = \frac{B'}{-C'}$, $F = \frac{F'}{-C'}$, $G = \frac{1}{-C'}$. Eqs. (5) below are the Gauss normal equations which provide the solution:

$$\begin{pmatrix} 1_{i_j}x_{i_j}^4 & x_{i_j}^2 y_{i_j}^2 & x_{i_j}^2 y_{i_j} \\ x_{i_j}^2 y_{i_j}^2 & 1_{i_j} y_{i_j}^4 & 1_{i_j} y_{i_j}^3 \\ x_{i_j}^2 y_{i_j} & 1_{i_j} y_{i_j}^3 & 1_{i_j} y_{i_j}^2 \end{pmatrix} \begin{pmatrix} B' \\ C' \\ F' \end{pmatrix} = \begin{pmatrix} -1_{i_j}x_{i_j}^2 \\ -1_{i_j}y_{i_j}^2 \\ -1_{i_j}y_{i_j} \end{pmatrix} \qquad (5)$$

Similarly, we calculate **H**, the hyperbola regression curve of $\mathcal{B}$, and we obtain the following equation Eq. (6) in the reference system $\mathcal{G}$ (Figure 4):

$$\mathbf{H} \equiv y = \frac{1}{2}F - \frac{1}{2}\sqrt{F^2 + 4Bx^2 + 4G}, B > 0 \text{ where } \begin{cases} B = 512.8713 \\ F = 252.01636 \\ G = -675.1128 \end{cases} \qquad (6)$$

This hyperbola regression curve $\mathbf{H} \equiv y = \frac{1}{2}F - \frac{1}{2}\sqrt{F^2 + 4Bx^2 + 4G}, B > 0$ is the one which best fits the point cloud $\mathcal{B} = \left\{P_{i_j}\right\}_{i_j=1}^{i_j=100}$, minimizing the sum of the quadratic residues $\sum_{i_j=1}^{i_j=100} \varepsilon_{hi_j}^2 = \sum_{i_j=1}^{i_j=100} \left(Bx_{i_j}^2 - y_{i_j}^2 + Fy_{i_j} + G\right)^2$, $B > 0$. The solution to this problem is not given by the Gauss normal equations, but by a critical point calculation. Eqs. (7) below are the critical point equations which provide the solution:

$$\begin{cases} \frac{\partial}{\partial B}\left(H(B,F,G)\right) = 0 \\ \frac{\partial}{\partial F}\left(H(B,F,G)\right) = 0 \\ \frac{\partial}{\partial G}\left(H(B,F,G)\right) = 0 \end{cases} \text{where } H(B,F,G) = \sum_{i_j=1}^{i_j=100} \left(\frac{1}{2}F - \frac{1}{2}\sqrt{F^2 + 4Bx_{i_j}^2 + 4G} - y_{i_j}\right)^2 \qquad (7)$$

In order to solve the above equations, we use the three-dimensional Newton-Raphson iteration with an accuracy of 10^{-6}. See Eq. (8) below:

$$\begin{pmatrix} B_{n+1} \\ F_{n+1} \\ G_{n+1} \end{pmatrix} = \begin{pmatrix} B_n \\ F_n \\ G_n \end{pmatrix} - \begin{pmatrix} \frac{\partial^2 H(B,F,G)}{\partial B^2} & \frac{\partial^2 H(B,F,G)}{\partial F \partial B} & \frac{\partial^2 H(B,F,G)}{\partial G \partial B} \\ \frac{\partial^2 H(B,F,G)}{\partial B \partial F} & \frac{\partial^2 H(B,F,G)}{\partial F^2} & \frac{\partial^2 H(B,F,G)}{\partial G \partial F} \\ \frac{\partial^2 H(B,F,G)}{\partial B \partial G} & \frac{\partial^2 H(B,F,G)}{\partial F \partial G} & \frac{\partial^2 H(B,F,G)}{\partial G^2} \end{pmatrix}_{(B_n,F_n,G_n)}^{-1} \begin{pmatrix} \frac{\partial H(B,F,G)}{\partial B}(B_n, F_n, G_n) \\ \frac{\partial H(B,F,G)}{\partial F}(B_n, F_n, G_n) \\ \frac{\partial H(B,F,G)}{\partial G}(B_n, F_n, G_n) \end{pmatrix} \qquad (8)$$

As the starting point we use (B_0, F_0, G_0), the coordinates of which are the coefficients of the above calculated equation for **E**, changing the sign of coefficient B. To that effect, we have developed our own numerical calculation software.

After all of the above, we have found out which conical curves show the best regression fit to the cloud B. Now we continue with the following hyperbolic curves:

We calculate **CH**, the hyperbolic cosine regression curve of B, and we obtain the following equation Eq. (9) in the reference system $\mathcal{G}$ (Figure 4):

$$\mathbf{CH} \equiv y = Acosh(x) + B \text{ where } \begin{cases} A = -3.8782 \\ B = 6.5757 \end{cases} \quad (9)$$

This hyperbolic cosine regression curve $\mathbf{CH} \equiv y = Acosh(x) + B$ is the one which best fits the point cloud $\mathcal{B} = \left\{P_{i_j}\right\}_{i_j=1}^{i_j=100}$, minimizing the sum of the quadratic residues $\sum_{i_j=1}^{i_j=100} \varepsilon_{hi_j}^2 = \sum_{i_j=1}^{i_j=100}\left(Acos\left(x_{i_j}\right) + B - y_{i_j}\right)^2$. Eqs. (10) below are the Gauss normal equations which provide the solution:

$$\begin{pmatrix} 1_{i_j}cosh^2\left(x_{i_j}\right) & 1_{i_j}cosh\left(x_{i_j}\right) \\ 1_{i_j}cosh\left(x_{i_j}\right) & 1_{i_j}1_{i_j} \end{pmatrix}\begin{pmatrix} A \\ B \end{pmatrix} = \begin{pmatrix} cosh\left(x_{i_j}\right)y_{i_j} \\ 1_{i_j}y_{i_j} \end{pmatrix} \quad \text{Eq. (10)}$$

Similarly, we calculate **C**, the catenary regression curve of $\mathcal{B}$, and we obtain the following equation Eq. (11) in the reference system $\mathcal{G}$ (Figure 4):

$$\mathbf{C} \equiv y = Acosh\left(\frac{x}{A}\right) + B \text{ where } \begin{cases} A = -0.3739 \\ B = 3.0265 \end{cases} \quad (11)$$

This catenary regression curve $\mathbf{C} \equiv y = Acosh\left(\frac{x}{A}\right) + B$ is the one which best fits the point cloud $\mathcal{B} = \left\{P_{i_j}\right\}_{i_j=1}^{i_j=100}$, minimizing the sum of the quadratic residues $\sum_{i_j=1}^{i_j=100} \varepsilon_{ci_j}^2 = \sum_{i_j=1}^{i_j=100}\left(Acosh\left(\frac{x_{i_j}}{A}\right) + B - y_{i_j}\right)^2$. Eqs. (12) below, where $W = \frac{1}{A}$, are the critical point equations which provide the solution:

$$\begin{cases} \frac{\partial}{\partial W}\left(C(W,B)\right) = 0 \\ \frac{\partial}{\partial W}\left(C(W,B)\right) = 0 \end{cases} \text{ where } C(W,B) = \sum_{i_j=1}^{i_j=100}\left(\frac{1}{W}cosh\left(Wx_{i_j}\right) + B - y_{i_j}\right)^2 \quad (12)$$

In order to solve the above equations, we use the three-dimensional Newton-Raphson iteration with an accuracy of 10^{-6}. See Eq. (13) below:

$$\begin{pmatrix} W_{n+1} \\ B_{n+1} \end{pmatrix} = \begin{pmatrix} W_n \\ B_n \end{pmatrix} = \begin{pmatrix} \frac{\partial^2 C(W,B)}{\partial W^2} & \frac{\partial^2 C(W,B)}{\partial B \partial W} \\ \frac{\partial^2 C(W,B)}{\partial W^2} & \frac{\partial^2 C(W,B)}{\partial B^2} \end{pmatrix}_{(W_n,B_n)}^{-1} \begin{pmatrix} \frac{\partial C(W,B)}{\partial W}(W_n, B_n) \\ \frac{\partial C(W,B)}{\partial W}(W_n, B_n) \end{pmatrix} \quad (13)$$

As the starting point we use $(W_0, B_0) = (A, B)$, the coordinates of which are the coefficients of the above calculated equation for $\mathbf{CH} \equiv y = Acosh(x) + B$. To that effect, we have developed our own numerical calculation software.

Finally, we calculate **R**, the Rankine regression curve of $\mathcal{B}$, and we obtain the following equation Eq. (14) in the reference system $\mathcal{G}$ (Figure 4):

$$\mathbf{R} \equiv y = Acosh(Cx) + B \text{ where } \begin{cases} A = -0.0325 \\ B = 2.5421 \\ C = 5.1012 \end{cases} \quad (14)$$

The classic Rankine's expression is: $y = Acosh\left(x\frac{2}{l}arccosh\left(\frac{A+h}{A}\right)\right) + B$, where l and h are the clear span and the height, respectively, of curve **R** on the reference system ⍰. Thus, for **R** we find that: $\frac{2}{l}arccosh\left(\frac{A+h}{A}\right) = 5.1012$.

We point out as follows: We do not call **R** a flattened catenary curve because it is not a catenary curve. We do not call it a general hyperbolic cosine curve either because it is not a hyperbolic cosine, but the analytical composition of a hyperbolic cosine with a homothetic transformation. We do not call it a funicular curve either because it does not correspond with the line obtained by hanging a finite number of weights from a chain.

This Rankine regression curve $\mathbf{R} \equiv y = Acosh(Cx) + B$ is the one which best fits the point cloud $\mathcal{B} = \left\{P_{i_j}\right\}_{i_j=1}^{i_j=100}$, minimizing the sum of the quadratic residues $\sum_{i_j=1}^{i_j=100} \varepsilon_{ri_j}^2 = \sum_{i_j=1}^{i_j=100}\left(Acosh\left(Cx_{i_j}\right) + B - y_{i_j}\right)^2$. Eqs. (15) below are the critical point equations which provide the solution:

$$\begin{cases} \frac{\partial}{\partial A}\left(R(A,B,C)\right) = 0 \\ \frac{\partial}{\partial A}\left(R(A,B,C)\right) = 0 \text{ where } R(A,B,C) = \sum_{i_j=1}^{i_j=100}\left(Acosh\left(Cx_{i_j}\right) + B - y_{i_j}\right)^2 \\ \frac{\partial}{\partial A}\left(R(A,B,C)\right) = 0 \end{cases} \quad (15)$$

In order to solve the above equations, in principle we would use the three-dimensional Newton-Raphson iteration with an accuracy of 10^{-6}. See Eq. (16) below:

$$\begin{pmatrix} A_{n+1} \\ B_{n+1} \\ C_{n+1} \end{pmatrix} = \begin{pmatrix} A_n \\ B_n \\ C_n \end{pmatrix} - \begin{pmatrix} \frac{\partial^2 R(A,B,C)}{\partial A^2} & \frac{\partial^2 R(A,B,C)}{\partial B \partial A} & \frac{\partial^2 R(A,B,C)}{\partial C \partial A} \\ \frac{\partial^2 R(A,B,C)}{\partial A \partial B} & \frac{\partial^2 R(A,B,C)}{\partial B^2} & \frac{\partial^2 R(A,B,C)}{\partial C \partial B} \\ \frac{\partial^2 R(A,B,C)}{\partial A \partial C} & \frac{\partial^2 R(A,B,C)}{\partial B \partial C} & \frac{\partial^2 R(A,B,C)}{\partial C^2} \end{pmatrix}_{(A_n,B_n,C_n)}^{-1} \begin{pmatrix} \frac{\partial R(A,B,C)}{\partial A}(A_n,B_n,C_n) \\ \frac{\partial R(A,B,C)}{\partial B}(A_n,B_n,C_n) \\ \frac{\partial R(A,B,C)}{\partial C}(A_n,B_n,C_n) \end{pmatrix} \quad (16)$$

In that case, we would use (A_0, B_0, C_0) as a starting point. However, this is not a stable convergent iteration.

But the above iteration is equivalent to the following stable convergent double iteration process. See Eqs. (17-29):

$$\begin{pmatrix} A_{n+1} \\ B_{n+1} \\ C_{n+1} \end{pmatrix} = \begin{pmatrix} A_n \\ B_n \\ C_n \end{pmatrix} - \begin{pmatrix} R_{11}(A_n,B_n,C_n) & R_{21}(A_n,B_n,C_n) & R_{31}(A_n,B_n,C_n) \\ R_{12}(A_n,B_n,C_n) & R_{22}(A_n,B_n,C_n) & R_{32}(A_n,B_n,C_n) \\ R_{13}(A_n,B_n,C_n) & R_{23}(A_n,B_n,C_n) & R_{33}(A_n,B_n,C_n) \end{pmatrix}^{-1} \begin{pmatrix} R_1(A_n,B_n,C_n) \\ R_2(A_n,B_n,C_n) \\ R_3(A_n,B_n,C_n) \end{pmatrix} (17),$$

where;

$$R_1(A_n,B_n,C_n) = \left(A_n \cosh\left(C_n x_{i_j}\right) + B_n - y_{i_j}\right)\cosh\left(C_n x_{i_j}\right) \quad (18)$$

$$R_2(A_n,B_n,C_n) = 1_{i_j}(A_n \cosh\left(C_n x_{i_j}\right) + B_n - y_{i_j}) \quad (19)$$

$$R_2(A_n,B_n,C_n) = \left(A_n \cosh\left(C_n x_{i_j}\right) + B_n - y_{i_j}\right)\sinh\left(C_n x_{i_j}\right) \quad (20)$$

$$R_{11}(A_n,B_n,C_n) = 1_{i_j}cosh^2\left(C_n x_{i_j}\right) \quad (21)$$

$$R_{21}(A_n, B_n, C_n) = 1_{i_j} cosh\left(C_n x_{i_j}\right) \qquad (22)$$

$$R_{31}(A_n, B_n, C_n) = x_{i_j} \sinh\left(C_n x_{i_j}\right)\left(2A_n \cosh\left(C_n x_{i_j}\right) + B_n - y_{i_j}\right) \qquad (23)$$

$$R_{12} = 1_{i_j} cosh\left(C_n x_{i_j}\right) \qquad (24)$$

$$R_{22}(A_n, B_n, C_n) = 1_{i_j} 1_{i_j} \qquad (25)$$

$$R_{32}(A_n, B_n, C_n) = x_{i_j} A_n\, sinh\left(C_n x_{i_j}\right) \qquad (26)$$

$$R_{13}(A_n, B_n, C_n) = x_{i_j} cosh\left(C_n x_{i_j}\right) sinh\left(C_n x_{i_j}\right) \qquad (27)$$

$$R_{23}(A_n, B_n, C_n) = x_{i_j} sinh\left(C_n x_{i_j}\right) \qquad (28)$$

$$R_{33}(A_n, B_n, C_n) = x_{i_j}^2\left(2A_n cosh^2\left(C_n x_{i_j}\right) - A_n + B_n \cosh\left(C_n x_{i_j}\right) - y_{i_j} \cosh\left(C_n x_{i_j}\right)\right) \qquad (29)$$

The formulas for the first iteration are those described above (17-29), but replacing the above equation (23) by the following equation: $R_{31}(A_n, B_n, C_n) = x_{i_j} sinh\left(C_n x_{i_j}\right)\left(2\cosh\left(C_n x_{i_j}\right) + B_n - y_{i_j}\right)$. As a starting point for this first iteration we use $X_{00} = (A_{00}, B_{00}, 1)$, the first two coordinates of which are the coefficients of the above calculated equation $\mathbf{H} \equiv y = Acosh(x) + B$. The formulas for the second iteration are those described above (17-29) with no changes. As a starting for the second iteration we use $X_0 = (A_0, B_0, C_0)$, which is the result of the first iteration.

After all of the above, we have obtained the specific analytic equations of the normalized regression curves **P**, **E**, **H**, **CH**, **C** and **R** for the cloud $\mathcal{B}$ corresponding to the edge of the access door to Palau Güell. These curves are shown in Figure 4.

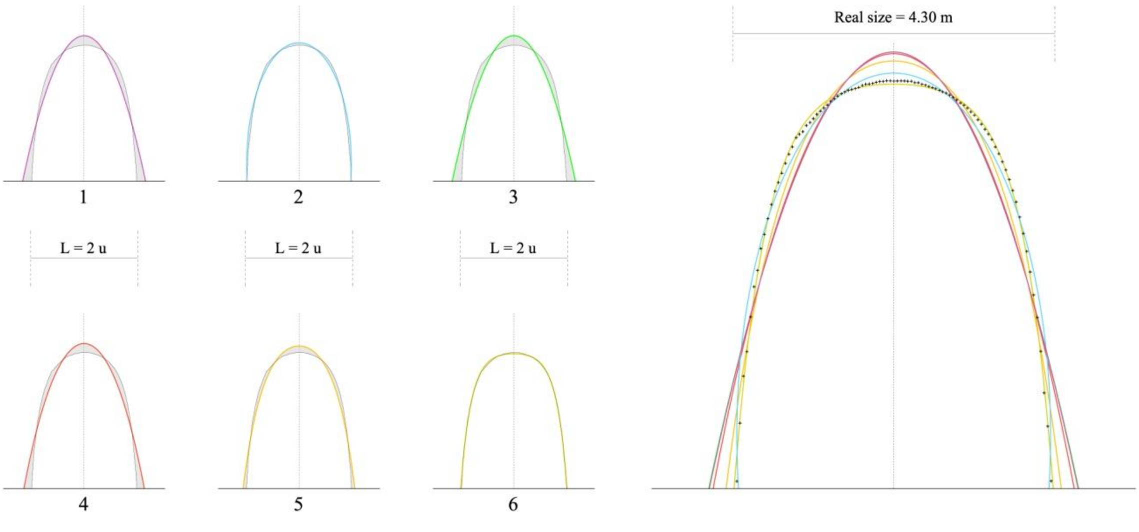

Fig. 4. The graphics on the left are sequentially numbered in correspondence with the following regression curves: parabola, ellipse, hyperbola, hyperbolic cosine, catenary and Rankine curve. The graphic on the right shows the cloud $\mathcal{B} = \left\{P_{i_j}\right\}_{i_j=1}^{i_j=100}$ and the superposition of the six curves obtained.

2.2. Statistical determination

Next we will calculate to what extent each of these curves statistically explains the cloud $\mathcal{B}$. For these calculations, we will use Pearson's coefficient of determination η^2, see Eq. (30):

$$\eta^2 = 1 - \frac{\sum_{i_j=1}^{i_j=100}\left(y_{i_j} - f\left(x_{i_j}\right)\right)^2}{\sum_{i_j=1}^{i_j=100}\left(y_{i_j} - \bar{Y}\right)^2} \qquad (30)$$

Where $\bar{Y} = \frac{1}{100}\sum_{i_j=1}^{i_j=100} y_{i_j}$, and where $\left(x_{i_j}, f\left(x_{i_j}\right)\right)$ are the coordinates of a point of the corresponding regression curve **P**, **E**, **H**, **CH**, **C** or **R**. Pearson's adjusted coefficient of determination η_{adj}^2 is given by Eq. (31):

$$\eta_{adj}^2 = 1 - [(1-\eta^2)]\,\frac{100-1}{100-d_1-1} \qquad (31)$$

Where d_1 is the number of parameters of the chosen regression curve. $\eta_{adj}^2 \in [0,1]$ in all cases, and the value $\eta_{adj}^2 * 100$ is the proportion in which the variable y_{i_j} of cloud $\mathcal{B}$ is statistically explained by the least-squares correlation between y_{i_j} and x_{i_j}. In other words, this value indicates the percentage of the variable y_{i_j} of cloud $\mathcal{B}$ which is statistically explained by the corresponding regression curve.

Table 1 below shows the results of the calculations for $\eta_{adj}^2 * 100$ in each regression model.

Model	$\boldsymbol{\eta_{adj}^2 * 100}$
P $\equiv \boldsymbol{y = Ax^2 + B}$	89.99
E $\equiv \boldsymbol{y = \frac{1}{2}F \pm \frac{1}{2}\sqrt{F^2 + 4Bx^2 + 4G}, B} < 0$	97.82
H $\equiv \boldsymbol{y = \frac{1}{2}F - \frac{1}{2}\sqrt{F^2 + 4Bx^2 + 4G}, B > 0}$	89.88
CH $\equiv \boldsymbol{y = A\cosh(x) + B}$	91.11
C $\equiv \boldsymbol{y = A\cosh\left(\frac{x}{A}\right) + B}$	95.71
R $\equiv \boldsymbol{y = A\cosh(Cx) + B}$	99.72

Table 1. Results of the calculations for $\eta_{adj}^2 * 100$ in each of the six regression models.

If a much more in-depth geometric analysis is to be made, all the calculations can be repeated not for the whole arch, i.e. the whole cloud $\mathcal{B}$, but for different arch segments. We explain this more precisely: We find the highest ordinate point y_{i_j} in $\mathcal{B}$ and the lowest ordinate point y_{i_j} in $\mathcal{B}$. The absolute difference d between both ordinate values is normalized to 1, so that 1 determines the whole cloud, while 0 determines only the highest point of the arch, and $t \in [0,1]$ determines the arch which is made up by all the points the height of which is greater than $1-t$. To put it more simply: we consider arch segments from top to bottom.

Now, for each $t \in [0,1]$, the set of points of the arch which is determined by t is called subcloud $\mathcal{B}_t$. For each t, we repeat the above six regression curve calculations for the subcloud $\mathcal{B}_t$. For this calculation we use a self-created numerical calculation software. Thus, for each $t \in [0,1]$ we obtain the regression curves $\mathbf{P_t}$, $\mathbf{E_t}$, $\mathbf{H_t}$,, $\mathbf{CH_t}$, $\mathbf{C_t}$ and $\mathbf{R_t}$. For each of these curves, we calculate the percentage of the variable y_{i_j} of the cloud $\mathcal{B}_t$ which is statistically explained by the regression curve sub-t, i.e. we calculate $adj_t = \eta_{adj}^2 * 100$ for each regression curve $\mathbf{P_t}$, $\mathbf{E_t}$, $\mathbf{H_t}$,, $\mathbf{CH_t}$, $\mathbf{C_t}$ and $\mathbf{R_t}$.

For our calculations we have used 1000 parameters $t \in [0,1]$ in each model type, i.e. we calculate everything for each $t = \frac{n}{1000}$, where $n = 1 \div 1000$. Figure 5 summarizes the results of the above explained calculations. Of course, the endpoints of the lines in Figure 5 correspond to the values shown in Table 1.

By means of the procedure described in this paper, using only geometric tools and concepts –without resort to physical, constructive or structural tools and concepts–, we have found the best-fitting curve for the edge of the access door to Palau Güell, designed by Antoni Gaudí.

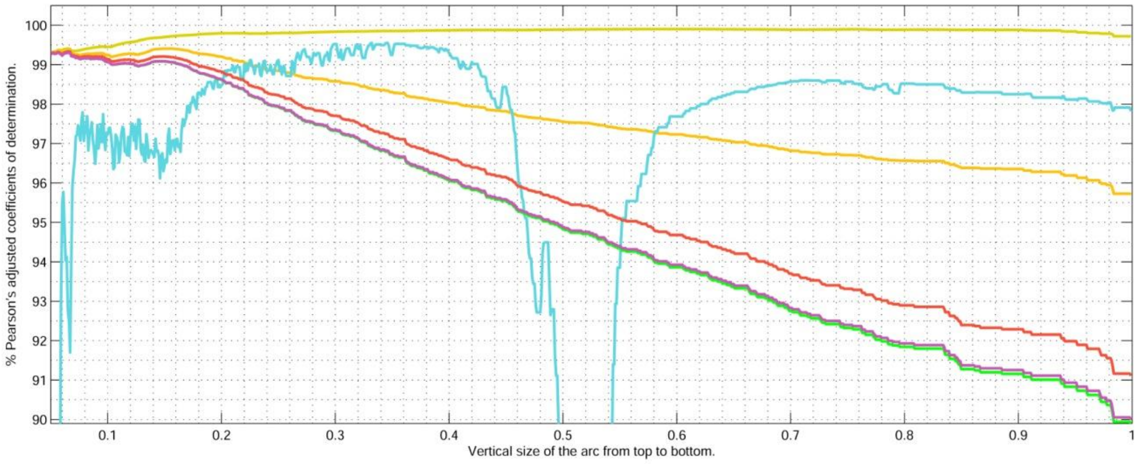

Fig. 5. Each point of the purple line has coordinates (t, adj_t), where adj_t is (Pearson's adjusted coefficient of determination)*100 for the curve $\mathbf{P}_t$; the same applies to the blue line and $\mathbf{E}_t$, the green line and $\mathbf{H}_t$, the red line and $\mathbf{CH}_t$, the orange line and $\mathbf{C}_t$, and the yellow line and $\mathbf{R}_t$.

3. Results

We have provided a mathematical process to objectively determine which is the geometric shape which best fits an arch of a heritage building within each of the conical curve types and hyperbolic curve types, and we have also provided an objective measurement of that fit. We have applied this method to the access door to Palau Güell, designed by Antoni Gaudí. We have provided the analytic equations for the best-fitting conical curves (ellipse, hyperbola and parabola) and hyperbolic curves (catenary, hyperbolic cosine and Rankine), and we have shown the percentage in which these curves statistically explain the analyzed arch.

We have normalized the size of the door, considering that an endpoint has coordinates $(1,0)$. In order to complete our paper, now we will show the reader how the equations change if the scale changes. More specifically, the equations for the regression curves **P**, **E**, **H**, **CH**, **C** and **R** have been calculated in the reference system $\mathcal{G} = \{\mathcal{v}; \vec{n}_1, \vec{n}_2\}$ –where the points have coordinates (x, y). Let us now assume that we want to find out the equations of the regression curves in the reference system $\vec{\mathcal{G}} = \{\mathcal{v}; \vec{m}_1 = K\vec{n}_1, \vec{m}_2 = K\vec{n}_2\}$, where $K \in \mathbb{R}^+$ and where the points have coordinates $(\tilde{x}, \tilde{y})$. In that case, the equations for each model are as follows:

$$\mathbf{P} \equiv \tilde{y} = \frac{A}{K}\tilde{x}^2 + KB \qquad (32)$$

$$\mathbf{E} \equiv \tilde{y} = \frac{1}{2}KF \pm \frac{1}{2}\sqrt{K^2F^2 + 4B\tilde{x}^2 + 4K^2G}, B < 0 \quad (33)$$

$$\mathbf{H} \equiv \tilde{y} = \frac{1}{2}KF \pm \frac{1}{2}\sqrt{K^2F^2 + 4B\tilde{x}^2 + 4K^2G}, B > 0 \quad (34)$$

$$\mathbf{CH} \equiv \tilde{y} = \tilde{A}cosh(\tilde{x}) + \tilde{B} \qquad (35)$$

$$\mathbf{C} \equiv \tilde{y} = KAcosh\left(\frac{\tilde{x}}{KA}\right) + KB \qquad (36)$$

$$\mathbf{R} \equiv \tilde{y} = KAcosh\left(\frac{C}{K}\tilde{x}\right) + KB \qquad (37)$$

In all cases, parameters A, B, C, F, G are the same as those which have already been calculated and provided for the normalized case; the only exception being the hyperbolic cosine curve **CH**, where the parameters $\tilde{A}$ and $\tilde{B}$ must be recalculated using the same method as for the normalized case.

Lastly, we note that we have used 100 points to define the edge cloud $\mathcal{B} = \left\{P_{i_j}\right\}_{i_j=1}^{i_j=100}$, which is a subcloud of the initial cloud $\mathcal{N}' = \{P'_i\}_{i=1}^{i=50155}$ having 50155 points. We could have used a higher number of points to determine the edge $\mathcal{B}$. However, a higher number of points does not significantly affect the calculation; the method to be used is exactly the same as described above, and the results are very much the same. The regression models are determined by those 100 points taken from the edge, and adding more points does not significantly change the regression.

4. Conclusions

Using standard geometric processes, numerical processes, computing, statistics and photogrammetrical data acquisition, we have provided a generic method to objectively determine which is the geometric shape which best fits an arch of a heritage building within each of the conical curve types and hyperbolic curve types, and we have also provided an objective measurement of that fit. In particular, we have used this method to determine the geometry of the access arch to Palau Güell, one of the most relevant buildings designed by Antoni Gaudí.

Contrary to the ambiguities and contradictions [2-5] regarding the geometric determination of this arch, as mentioned in the introduction to this paper, and also without using mechanical or structural tools and without resort to historical documents which might justify and clarify the arch type: from an infinite number of conical and hyperbolic curves, the method described lets us find those which best fit the access door to Palau Güell (with their specific parameters), and also provides a measure of that fit. In light of these results we see, among other things, that the best-fitting curve γ for that arch is a Rankine curve (Figure 6). While it is true that the author of publication [5] says that the access arch to Palau Güell "is very similar to" a Rankine curve, he does not specify how close that similarity is and he does not mention which particular Rankine curve he means. We also point out that for this paper we have only used geometric techniques, while publication [5] relies on structural and mechanical techniques.

In summary: from the infinite number of curves belonging to the six models considered –three conical curve models and three hyperbolic curve models–, the curve γ which best fits the access arch to Palau Güell –the real size of this arch is given by $K = 2.15m$ (Figure 4 and 6)– is the Rankine curve described by Eq. (38), with a 99.72% fit. Also, from the infinite number of curves of those six types, the no-Rankine curve δ which best fits the access door is the ellipse described by Eq. (39), with a 97.82% fit. Surprisingly enough, this has never been mentioned in previous papers. Finally, Figure 6 shows both curves in red and yellow, respectively.

$$\gamma \equiv\ y = KAcosh\left(\frac{C}{K}x\right) + KB \equiv\ y = -0.07cosh(2.37x) + 5.47 \qquad (38)$$

$$\delta \equiv y = \frac{1}{2}KF \pm \frac{1}{2}\sqrt{K^2F^2 + 4Bx^2 + 4K^2G} \equiv y = 0.72 \pm \frac{1}{2}\sqrt{93.28 - 21.29x^2} \qquad (39)$$

Fig. 6. Curve γ is shown in red over the study arch. Curve δ is shown in yellow. The four remaining regression curves (parabola, hyperbola, catenary and hyperbolic cosine curve) are shown in blue.

5. References

[1] S. Huerta, La teoría del arco de fábrica: desarrollo histórico, Obra pública (38) (1196) 18-29.

[2] D. Girant Miracle, et al, Gaudí, búsqueda de la forma: espacio, geometría, estructura y construcción, Lunwerg, Spain, 2002, pp. 97-102

[3] A. G. García, La organización constructiva del descenso de cargas del Palau Güell de Barcelona obra de Antoni Gaudí, Actas del Tercer Congreso Nacional de Historia de la Construcción, Sevilla, 26 a 28 de octubre de 2000. Instituto Juan de Herrera. Vol. I, pp. 443-450.

[4] E. Granell, El Palau Güell de Antoni Gaudí en Barcelona: 1886-1888. *DC PAPERS*, Revista de crítica y teoría de la arquitectura (7) (2002) 48-55.

[5] S. Huerta, Structural design in the work of Gaudí, Architectural Science Review 49 (4) (2206) 324-339.

Figure 1
Click here to download high resolution image

Figure 2
Click here to download high resolution image

Figure 3
Click here to download high resolution image

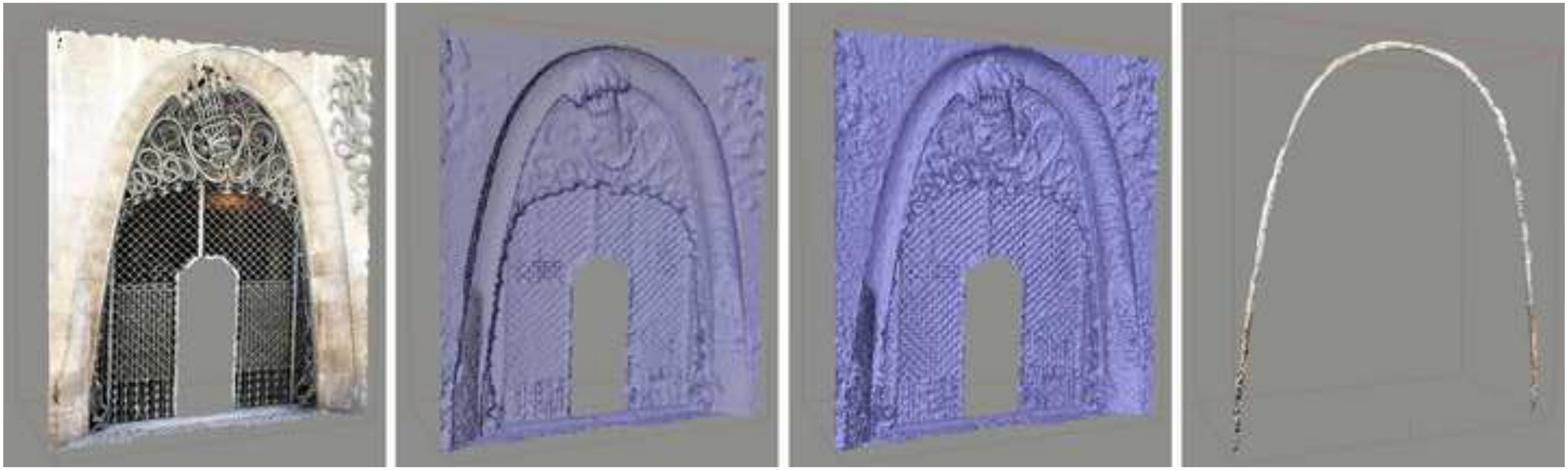

Figure 4
Click here to download high resolution image

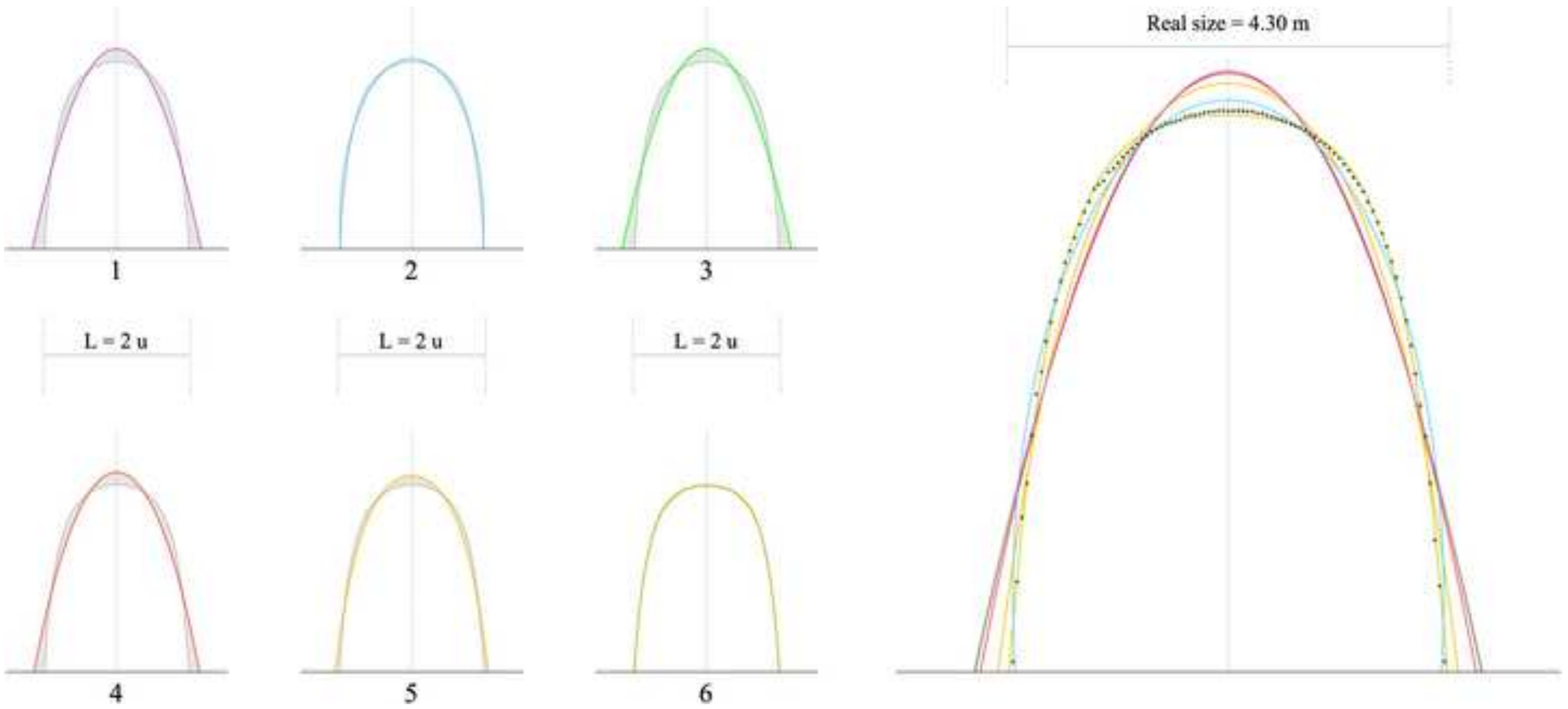

Figure 5

Click here to download high resolution image

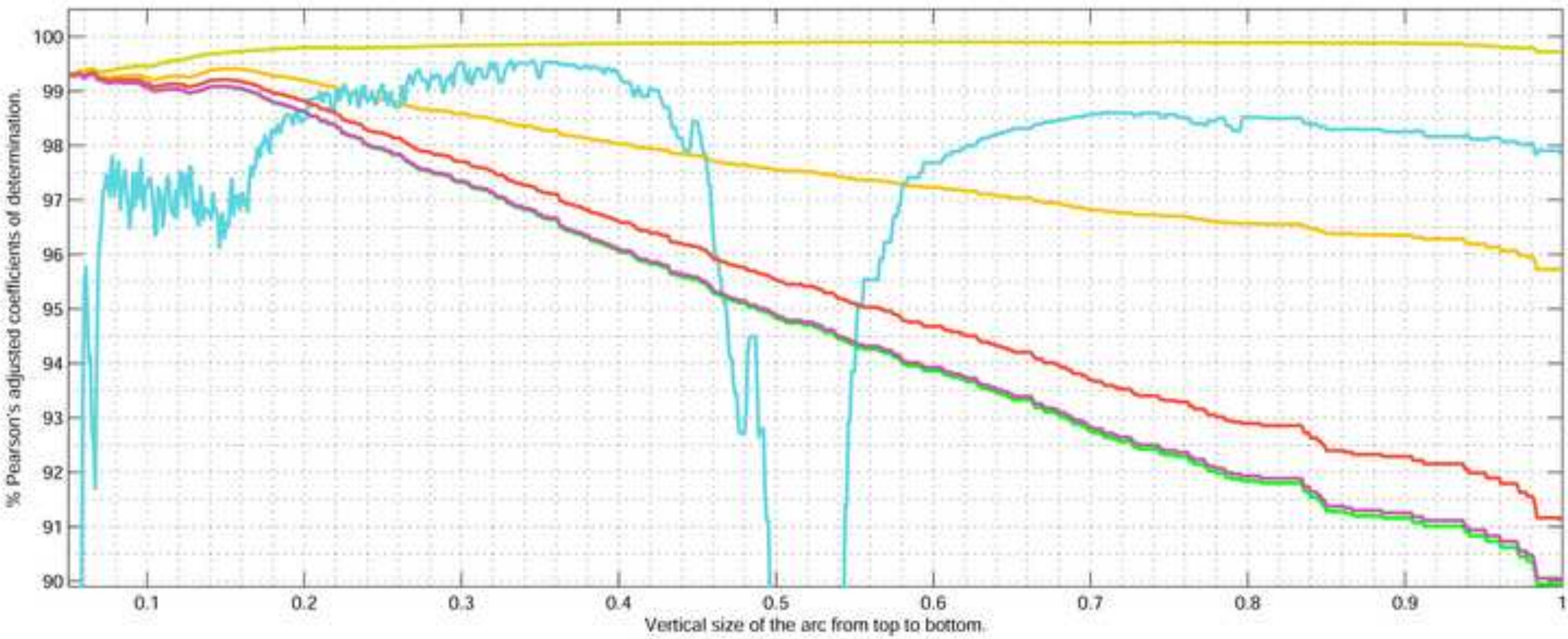

Figure 6
Click here to download high resolution image